Chemical Science Review and Letters ISSN 2278-6783

www.chesci.com Research Article

Comparative Study of Two Nitroimidazopyridinehydrazone Derivatives Inhibition Action for Aluminum Corrosion in 2M HCl: Experimental and Theoretical Insights

Mougo André Tigori[1]*, Kouassi Francesco Adingra[2], Aboudramane Koné[1], Cissé M'Bouillé[1], Drissa Sissouma[2], Paulin Marius Niamien[2]

[1]Laboratoire des Sciences et Technologies de l'Environnement, UFR Environnement, Université Jean Lorougnon Guédé, BP 150 Daloa, Côte d'Ivoire

[2]Laboratoire de Constitution et de Réaction de la Matière, UFR SSMT, Université Félix Houphouët-Boigny, 22 BP 582 Abidjan 22, Côte d'Ivoire

Abstract

The aim of this work is to study the inhibition performance of 2-benzylidene-1-(3-nitro H-imidazo[1,2-a]pyridin-2-yl)hydrazine (BNIH) and 2-(2-nitrobenzylidene)-1-(3-nitro H-imidazo[1,2-a]pyridin-2-yl)hydrazine (NBIH) for aluminum corrosion in 2M HCl. This study was carried out using experimental methods and theoretical calculations. Mass loss techniques indicate that BNIH has a greater inhibition effect than NBIH, with inhibition efficiencies of 95.78% and 91.56% respectively at 298K and 0.8mM concentration. Adsorption of these compounds on aluminum surface follows Villamil model. This adsorption occurs in two ways: physisorption and chemisorption. Theoretical results obtained from Density Functional Theory (DFT)/B3LYP-6-31G(d,p) and Quantitative Structure-Property Relationship(QSPR) helped to explain the interactions between each inhibitor and aluminum. These interactions justify the results obtained experimentally. Furthermore, this work reported the NO_2 substituent effect in an organic compound.

Keywords: Aluminum, corrosion inhibitors, Mass loss techniques, Density Functional Theory, Quantitative Structure-Property Relationship

***Correspondence**

Author: Mougo André Tigori

Email: tigori20@yahoo.fr

Introduction

The search for effective, long-lasting treatments to protect metal equipment against corrosion has become a subject requiring a great deal of attention. Indeed, the protection of materials against this phenomenon consists in using techniques and treatments to reduce or prevent their degradation [1]. Corrosion affects many companies' economies in developed countries or underdeveloped countries [2]. In fact, these companies spend large sums of money to replace corroded equipment. In this context, the condition of metallic materials should be monitored during the cleaning operation in acidic solutions [3,4]. These acidic solutions promote metal structure oxidation. To guarantee safety and reduce environmental pollution, the search for ways to combat this scourge has become paramount. In recent years, several studies have been conducted in this field. These techniques aim to find low-toxicity molecules that are effective in slowing down the oxidation of metal structures during acid pickling operations [5]. Among these metal structures, aluminum, which is widely used because of its good physicochemical properties, corrodes easily [6]. This oxidation adversely affects the mechanical operation of aluminum components.

According to the literature, some organic and inorganic molecules have been tested and are shown to be effective against aluminum corrosion in an acidic medium [7-12]. These molecules adsorb to metal surfaces by reducing the loss of electrons in acidic media. The effectiveness of these compounds is linked to the presence in these molecules of aromatic rings and polar functions with heteroatoms O, N, S, and P [13].

Among various corrosion inhibitors studied, the drugs and synthetic molecules are the most widely used at present time. These compounds are generally effective, environmentally friendly, and of low toxicity [14-18].

In this study, two nitroimidazopyridinehydrazone derivatives will be evaluated for inhibition potential. The choice of these compounds is that little work appears to have been carried out in the field of aluminum corrosion inhibition using these derivatives. In addition, these derivatives have been used for the treatment of candidiasis and lung and pancreatic cancer [19,20]. Thus, these therapeutic compounds can not only preserve the environment and be ideal candidates for the protection of metals against corrosion.

The purpose of this work is to conduct a comparative study between 2-benzylidene-1-(3-nitro-H-imidazo[1,2-a]pyridine-2-yl)hydrazine and 2-(2-nitro benzylidene)-1-(3-nitro-H-imidazo[1,2-a]pyridin-2-yl)hydrazine for aluminum corrosion inhibition in 2M hydrochloric acid solution using gravimetric and theoretical techniques.

Theoretical studies based on Density Functional Theory (DFT) and the Quantitative Structure-Property Relationship (QSPR) are aimed at determining the relationship between quantum chemical parameters, compound structures, and experimentally determined inhibition efficiencies. Finally, the theoretical aspect will contribute to finding the right parameters to characterize the experimental behavior of each compound.

Materials and Methods

Molecules synthesis procedure

Inhibitor molecules were synthesized at the Laboratory of Constitution and Reaction of Matter of Felix Houphouet Boigny University. The synthesis procedure is explained in **Figure 1**. The molecular structures of these inhibitors are given in **Figure** 2.

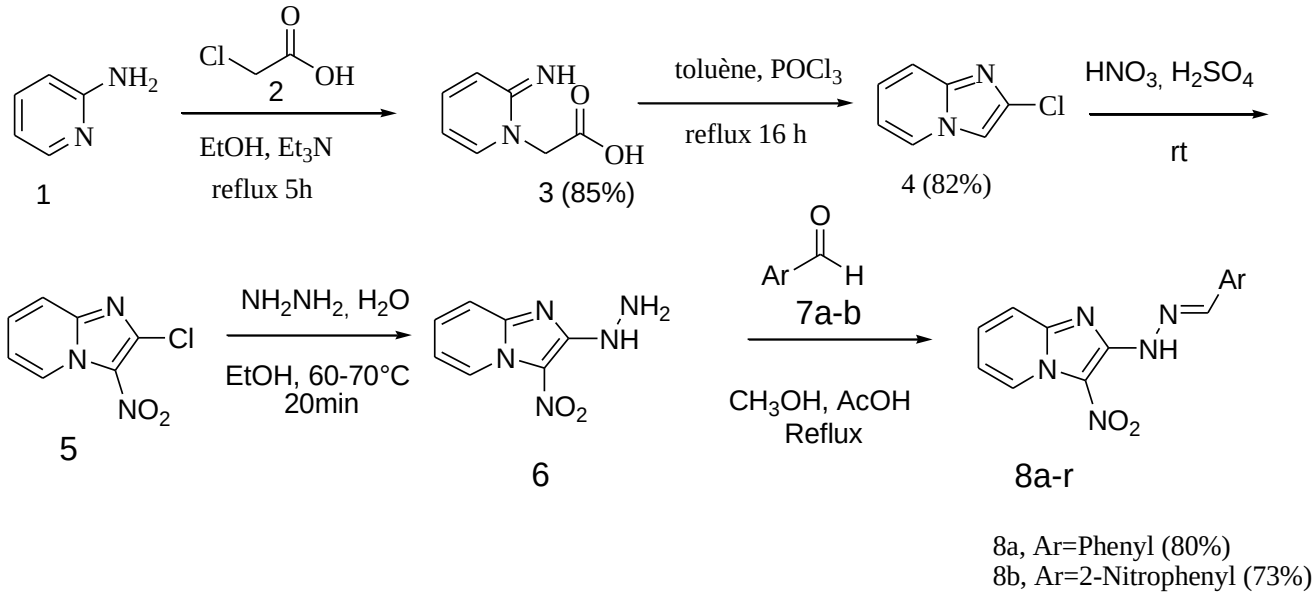

Figure 1 Inhibitor synthesis procedure

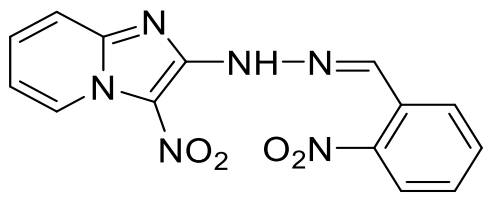

2-(2-nitrobenzylidene)-1-(3-nitro H-imidazo[1,2-a]pyridin-2-yl)hydrazine (8b): NBIH

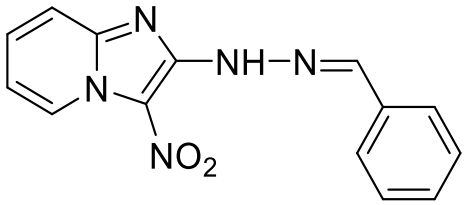

2-benzylidène-1-(3-nitro H-imidazo[1,2-a]pyridine-2-yl)hydrazine (8a): BNIH

Figure 2 The molecular structure of inhibitors tested

Solutions and aluminum samples preparation

A 2M hydrochloric acid solution was prepared from a commercial hydrochloric acid solution of purity 37%, density 1.19, and molar mass 36.46g/mol. This solution was used to prepare 0.1M, 0.3M, 0.6M, and 08M concentrations of BNIH and NBIH.

Aluminum samples of 99.8% purity, in the form of cylindrical rods measuring 10 mm long and 2 mm in diameter, were successively polished with fine-grade emery paper with grit sizes ranging from 120 to 600, cleaned with acetone, washed with bidistilled water, dried in a desiccator and finally weighed (m_1). An oven was used to dry the aluminum samples.

Gravimetric method

The mass loss techniques used in this study consist in monitoring the variation in the mass of an aluminum sample immersed for 1h in 2M hydrochloric acid solution with or without the inhibitors. After pre-treatment each sample was completely immersed for 1h in an Erlenmeyer flask containing 50 ml of 2M HCl with or without the different concentrations of each inhibitor. After this time, each sample was removed, washed again with double-distilled water, then dried and reweighed (m_2) using an analytical balance. Tests were repeated at temperatures ranging from 298K to 323K. The temperature was controlled by a thermostat water bath. The mass loss ($\Delta m = m_1-m_2$) is obtained by averaging three tests in each case.

This method provides access to quantities such as corrosion rates (W), surface coverage (θ), and inhibition efficiency IE (%). The expressions for these quantities are given by the following equations:

$$W = \frac{\Delta m}{S_e.t} = \frac{m_1-m_2}{S_e.t} \quad (1)$$

$$\theta = \frac{W_0-W}{W_0} \quad (2)$$

$$IE(\%) = \frac{W_0-W}{W_0} * 100 \quad (3)$$

Δm: is the mass loss (g) m_1 and m_2 are respectively, the mass (g) before and after immersion in the solution test; t is the immersion time (h) ;S_e is the total surface of the sample in cm^2 ; w_0 and w are respectively the copper corrosion rates in the absence and presence of BNIH and NBIH.

Theoretical calculation methodology

Density Functional Theory details

In this work, quantum chemical calculations and molecular structure optimization were performed with Gaussian 09 [21] software with density functional theory (DFT) using 6-31G (d, p) basis sets and B3LYP functional including three-parameter of Becke (B3): Lee, Yang, and Parr (LYP), which comprises a mixture of Hatree Fock and DFT exchange terms [22,23]. This theory (DFT) permits to determine global and local quantum chemical parameters such as the highest occupied molecular orbital energy (E_{HOMO}), the lowest unoccupied molecular orbital energy (E_{LUMO}), the energy gap (ΔE),the dipole moment (μ), the electron affinity (A), the ionization energy (I), the electronegativity (χ), the hardness (η), the softness (σ),the electrophylicity index (ω),the fraction of electron transferred (ΔN),the total energy (E_T), the Fukui functions (f_k^+, f_k^-), and the dual descriptor ($\Delta f_k(r)$). These parameters are determined from the expressions below [24, 25]:

$$\Delta E = E_{LUMO} - E_{HOMO} \quad (4)$$

$$I = -E_{HOMO} \quad (5)$$

$$A = -E_{\mathrm{LUMO}} \quad (6)$$

$$\chi = -\mu_p = \left(\frac{\partial E}{\partial N}\right)_{v(r)} \quad (7)$$

$$\chi = \frac{I+A}{2} \quad (8)$$

$$\eta = \frac{I-A}{2} \quad (9)$$

$$\sigma = \frac{1}{\eta} = \frac{2}{I-A} \quad (10)$$

$$\omega = \frac{\mu_P^2}{2\eta} = \frac{(I+A)^2}{4(I-A)} \quad (11)$$

$$\Delta N = \frac{\phi_{Al}-\chi_i}{2(\eta_{Al}+\eta_i)} \quad (12)$$

Where ϕ_{Al}= 4.28 eV [23] and the hardness of copper η_{Al}= 0 [26], χ_i and represents the electronegativity and the η_i hardness of each inhibitor molecule.

$$f_k^+ = [q_k(N+1) - q_k(N)] \quad (13)$$

$$f_k^- = [q_k(N) - q_k(N-1)] \quad (14)$$

Where f_k^+ and f_k^- are respectively nucleophilic and electrophilic Fukui functions, $q_k(N+1)$, $q_k(N)$, and $q_k(N-1)$ are the atomic charges of the systems with $N+1$, N, and $N-1$ electrons population, respectively [27].

The dual descriptor has been associated with Fukui functions for unambiguous identification of reactivity sites within each inhibitor [28, 29]. This parameter is expressed according to the following equation:

$$\Delta f_k(r) = f_k^+ - f_k^- \quad (15)$$

Quantitative Structure-Property Relationship (QSPR) calculations

To find a mathematical relationship between experimental inhibition efficiency and quantum chemical parameters, a quantitative structure-property relationship approach was used in this study [30]. The relationships obtained from this model can be used to predict inhibition efficiency from compound concentrations. This prediction relates to the behavior of each inhibitor at a metal surface in a corrosive solution. In this work, the linear model proposed by Lukovits et *al* was used [31]. This model is expressed as follows:

$$IE_{calc}(\%) = \frac{[Ax_j+B]C_i}{1+[Ax_j+B]C_i} * 100 \quad (16)$$

Where C_i represents the concentrations of the inhibitors used, x_j are global chemical parameters, and A, B are real constants.

This approach is validated utilizing of the determination coefficient (R^2) and statistical parameters expressed as follows:

- the sum of square errors (SSE),

$$\mathrm{SSE} = \sum_{i=1}^{N}\left(\mathrm{IE_{exp}} - \mathrm{IE_{calc}}\right)^2 \quad (17)$$

- the root mean square error (RMSE),

$$\mathrm{RMSE} = \sqrt{\frac{\sum_{i=1}^{N}\left(\mathrm{IE_{exp}}-\mathrm{IE_{calc}}\right)^2}{N}} \quad (18)$$

Results and Discussion

Gravimetric analysis

Temperature and inhibitor concentration effect on corrosion rate

Figure 3 reports corrosion rate evolution as a function of temperature NBIH, and BNIH concentrations.

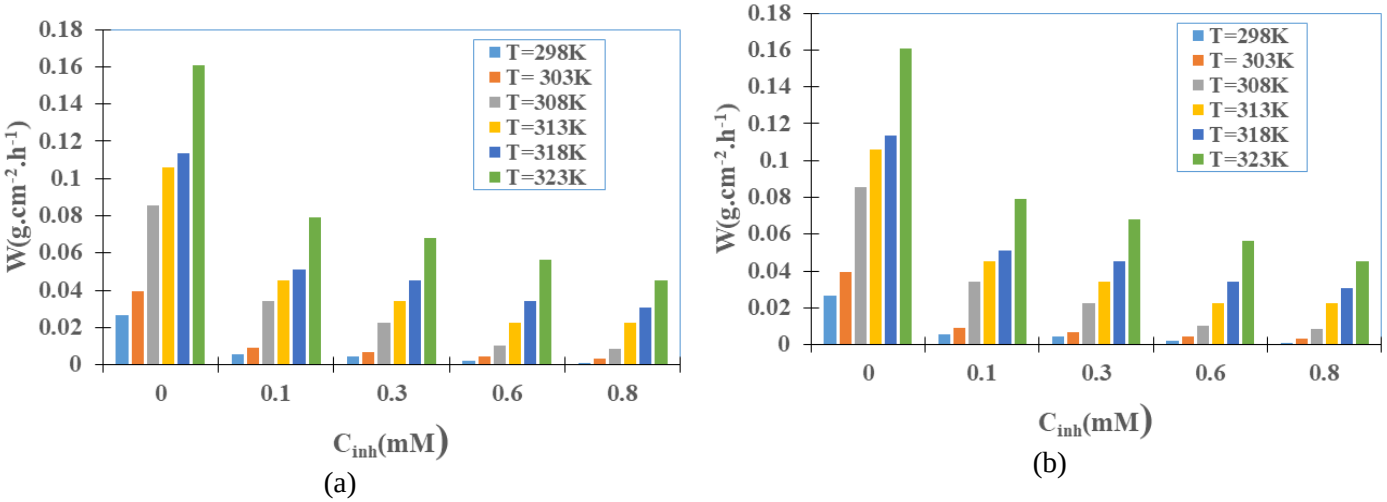

Figure 3 The corrosion rate versus concentration and temperature. (a) NBIH, (b) BNIH

Looking at this **Figure 3**, it is clear that the corrosion rate increases with temperature and decreases with increasing molecule concentration. It can be seen that the corrosion rate of BNIH decreases more than that of NBIH with increasing inhibitor concentration. In this case, increasing inhibitor concentration reduces the aluminum corrosion rate.

Temperature and inhibitor concentration effect on inhibition efficiency

Compound inhibition efficiency evolution as a function of temperature and the concentration of each inhibitor is described in **Figure 4**.

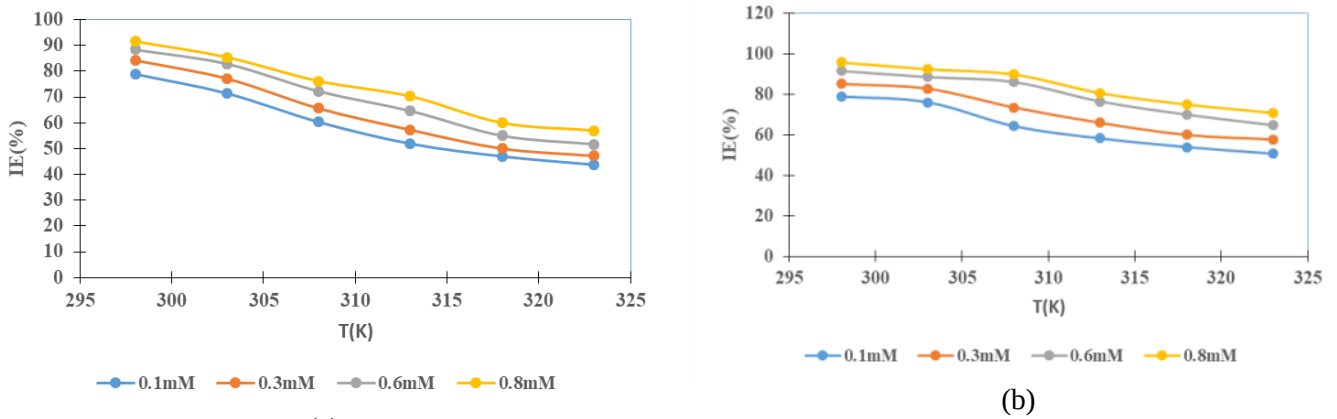

Figure 4 Inhibition efficiency versus concentration and temperature. (a) NBIH, (b) BNIH

Figures 4 examination reveals that the inhibition efficiency of each molecule decreases with increasing temperature. While an increase in inhibitor concentration is accompanied by a rise in inhibition efficiency. These results suggest that each inhibitor adsorption on the aluminum surface becomes less and less important as temperature evolves. Moreover, these observations can also be explained by the increasing solubility of protective films and corrosion products initially precipitated on the metal surface, progressively exposing the aluminum surface to attack by aggressive solution as the temperature rises. In addition, higher inhibitor concentrations increase the coverage of the metal surface, which slows aluminum dissolution in aggressive solution, thus justifying the increase in inhibition efficiency. Similar results have been obtained by previous works [32, 33].

Adsorption isotherms and thermodynamic parameters investigation

Gravimetric analysis indicates that the compounds studied absorb strongly to metal surfaces at base temperature. The adsorption isotherm that could explain the adsorptive behavior of each inhibitor must be sought. However, a series of isotherm models have been tested, namely Langmuir, Temkin, Freundlich, El-Awady, and Frumkin isotherms, to find the most suitable model. The expressions for these different isotherms are given by the following equations:

$$\text{Langmuir}: \quad \frac{C_{inh}}{\theta} = \frac{1}{K_{ads}} + C_{inh} \qquad (19)$$

$$\text{Temkin}: \theta = \frac{2.303}{f}[logK_{ads} + logC_{inh}] \qquad (20)$$

$$\text{El-Awady}: log(\theta/1-\theta) = logK + ylogC_{inh} \qquad (21)$$

$$\text{Freunlich}: log\theta = logK + nlogC_{inh} \qquad (22)$$

$$\text{Frumkin}: \frac{\theta}{1-\theta}\exp(-2f\theta) = k_{ads}C_{inh} \qquad (23)$$

For all the models tested, Langmuir isotherm is the most appropriate and best reflects the absorptive behavior of each inhibitor on the aluminum surface. Indeed, the determination coefficients (R^2) of this isotherm are closer to unity than those of the others. **Figure 5** illustrates this isotherm for the various compounds studied.

The parameters of the straight lines of this isotherm are shown in **Table 1**. Although Langmuir isotherm has coefficients determination (R^2) very close to unity, the slopes of the lines obtained are greater than one. In this case, the appropriate model for this study is the modified Langmuir isotherm or Villamil model [34]. The applicability of this isotherm has enabled determination of the thermodynamic parameters using the following relationships [35]:

$$\Delta G^0_{ads} = -RTln(55.5K_{ads}) \qquad (24)$$

$$\Delta G^0_{ads} = \Delta H^0_{ads} - T\Delta S^0_{ads} \qquad (25)$$

Where ΔG^0_{ads} is free adsorption enthalpy change, K_{ads} is the adsorption equilibrium constant, 55.5 is the water concentration, R is the gas perfect constant and T is the absolute temperature. Adsorption enthalpy ΔH^0_{ads} and the

adsorption entropy ΔS^0_{ads} values have been deduced from straight line parameters obtained in **Figure 6**. Various thermodynamic adsorption parameter values are given in **Table 2**.

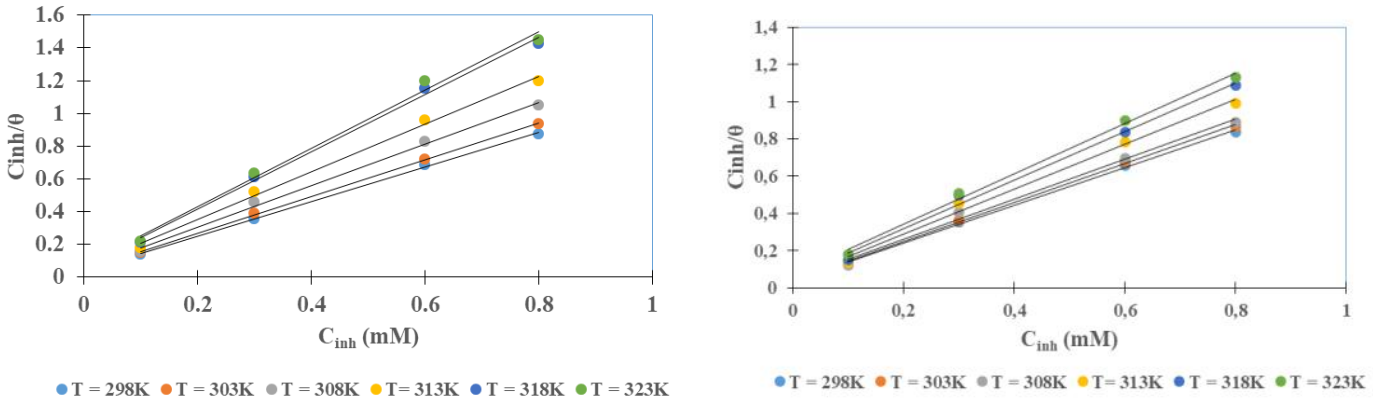

(a) (b)

Figure 5 Langmuir isotherm adsorption plotted as (a) NBIH, (b) BNIH

Table 1 Langmuir isotherm parameters of NBIH and BNIH

Compound	Temperature	Equations	R^2
NBIH	298	$\frac{C_{inh}}{\theta} = 1.0563C_{inh} + 0.0391$	0.999
	303	$\frac{C_{inh}}{\theta} = 1.1238C_{inh} + 0.0439$	0.9995
	308	$\frac{C_{inh}}{\theta} = 1.2724C_{inh} + 0.0509$	0.9963
	313	$\frac{C_{inh}}{\theta} = 1.4569C_{inh} + 0.0605$	0.9995
	318	$\frac{C_{inh}}{\theta} = 1.7451C_{inh} + 0.0671$	0.9955
	323	$\frac{C_{inh}}{\theta} = 1.7811C_{inh} + 0.0752$	0.9921
BNIH	298	$\frac{C_{inh}}{\theta} = 1.0118C_{inh} + 0.0371$	0.9982
	303	$\frac{C_{inh}}{\theta} = 1.0468C_{inh} + 0.0385$	0.9987
	308	$\frac{C_{inh}}{\theta} = 1.0796C_{inh} + 0.0431$	0.9914
	313	$\frac{C_{inh}}{\theta} = 1.2066C_{inh} + 0.0483$	0.991
	318	$\frac{C_{inh}}{\theta} = 1.3047C_{inh} + 0.563$	0.9915
	323	$\frac{C_{inh}}{\theta} = 1.3501C_{inh} + 0.0718$	0.9949

Table 2 Analysis certifies that K_{ads} values for both inhibitors are high, decreasing with increasing temperature. The high values at base temperature confirm the strong adsorption of each inhibitor to the aluminum surface, leading to better inhibition performance of the compounds. Whereas the decreasing K_{ads} values indicate that adsorption is diminished with increasing temperature, justifying the low inhibition efficiencies obtained with increasing temperature. BNIH exhibits the highest K_{ads} values, demonstrating its good inhibition efficiency compared with NBIH.This poor performance of BNIH compared with NBIH could be justified by the presence of two NO_2 substituents in the NBIH structure. These observations may attest that NO_2 presence in an organic compound can influence its inhibition power towards metal corrosion.

Negative ΔG^0_{ads} values for both inhibitors relate the adsorption spontaneity to the metal surface [36]. These values are in the range of -20 kJ/mol to -40 kJ/mol notifying mixed adsorption: chemisorption and physisorption [37].

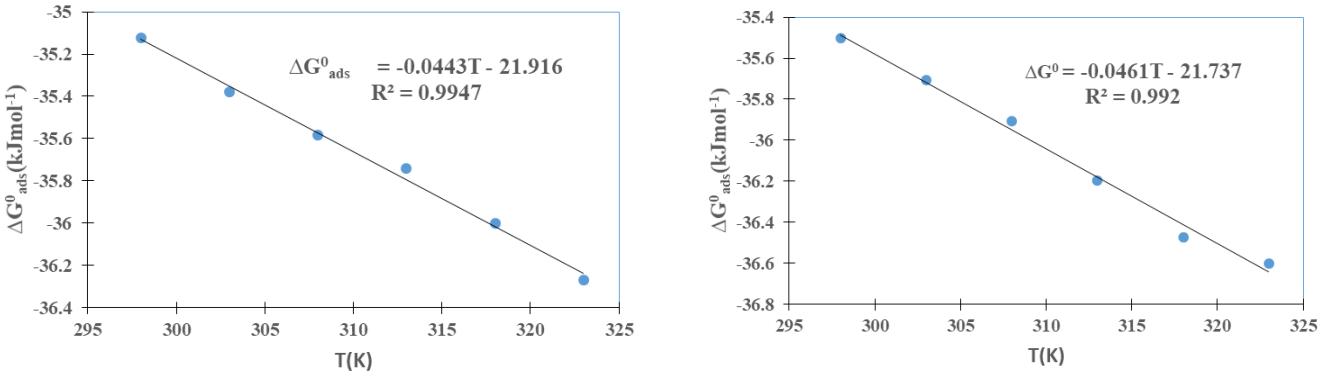

(a) (b)

Figure 6 Free adsorption enthalpy change versus temperature of (a) NBIH, (b) BNIH

Table 2 Adsorption equilibrium constant and thermodynamic adsorption parameters

Inhibitor	T(K)	K_{ads}	ΔG^0_{ads} ($kJ\ mol^{-1}$)	ΔH^0_{ads} ($kJ\ mol^{-1}$)	ΔS^0_{ads} ($J\ mol^{-1}K^{-1}$)
	298	25575.4476	-35.1220		
NBIH	303	22779.0433	-35.3769		
	308	19646.3654	-35.5820	-44.3	21.91
	313	16666.6667	-35.7318		
	318	14925.3731	-36.011		
	323	13297.8723	-36.2672		
	298	26954.1779	-35.5022		
	303	25974.02597	-35.7074		
BNIH	308	23201.85615	-35.9077	-46.1	21.73
	313	20703.93375	-36.1960		
	318	17761.98934	-36.4708		
	323	13927.5766	-36.6015		

Adsorption enthalpy (ΔH^0_{ads}) values are negative indicating an exothermic adsorption process. This adsorption characteristic confirms the physical and chemical adsorption presence for each inhibitor on the aluminum surface [36]. Whereas adsorption entropy (ΔS^0_{ads}) values are positive expressing the increase in disorder during the adsorption phenomenon of each inhibitor [38].

Activation parameters

The corrosion rate increases with increasing temperature, revealing that temperature influences on the corrosion process. To understand temperature influence in explaining the inhibition mechanism, thermodynamic activation parameters were determined. The relationship between corrosion rate and temperature is given by the Arrhenius equation, while an alternative form of the Arrhenius equation permits enthalpy and entropy of activation to be determined. These different equations are expressed as follows [35, 39]:

$$W = A.exp\left(-\frac{E_a}{R.T}\right) \quad (26)$$

$$\log\left(\frac{W}{T}\right) = \log\left(\frac{R}{N_A h}\right) + \frac{\Delta S^*_a}{2{,}303R} - \frac{\Delta H^*_a}{2{,}303RT} \quad (27)$$

Where W is the corrosion rate in the presence of inhibitor, E_a activation energy, R universal gas constant, A the frequency factor, h is Planck constant, N_A is Avogadro number, activation enthalpy ΔH^*_a, and activation entropy ΔS^*_a.

The thermodynamic activation parameters calculated are listed in **Table 2**. **Table 2** inspection reveals that for both compounds, the activation energy values in the uninhibited solution (blank) are lower than those in the inhibited solutions. These observations reveal that aluminum dissolves easily in inhibitor (NBIH or BNIH) absence in 2M hydrochloric acid solution. This dissolution becomes increasingly difficult in NBIH or BNIH presence as their concentration increases. As a result, the protective layer on the aluminum surface increases with inhibitor concentration. These results reflect the electrostatic interactions predominance between charged inhibitor molecules

and the charged metal surface (physisorption) [40]. This type of adsorption does not effectively reduce corrosion as the temperature rises. These pieces of information confirm the temperature-dependent decrease in inhibition efficiency, observed in experimental measurements.

The positive ΔH_a^* values confirm the endothermic nature of the metal dissolution reaction, so the inhibition mechanism is influenced by physical adsorption [41, 42]. ΔS_a^* values that increase from negative to positive values for both inhibitors indicate that activated complex formation in the rate-determining step is dissociative rather than associative in addition. These data can be interpreted as an increase in disorder during the transformation of the reactants into the activated complex [42].

Table 2 Activation parameters

Inhibitor	Concentration(mM)	$E_a(kJmol^{-1})$	$\Delta H_a^*(kJmol^{-1})$	$\Delta S_a^*(Jmol^{-1}K^{-1})$
	0	61.2902	69.8666	-40.6754
	0.1	87.8358	85.2548	-0.2105
NBIH	0.3	97.8321	95.2510	30.6941
	0.6	112.4691	113.6571	87.9299
	0.8	115.0405	116.7650	93.3645
	0	61.2902	69.8666	-40.6755
BNIH	0.1	91.0510	83.3138	-7.2813
	0.3	94.2987	87.6346	4.5926
	0.6	105.6803	103.0993	50.6530
	0.8	119.5280	116.9470	93.0775

Quantum chemical parameters analysis

The correlation between quantum chemical parameters and experimental data was carried out on DFT calculations and gravimetric results basis. Global chemical parameters of the inhibitors derived from DFT calculations are listed in **Table 3**.

Table 3 Global Reactivity Descriptors for BNIH and NBIH with B3LYP/ 6-31G(d,p)

Quantum chemical parameters	NBIH	BNIH
E_{HOMO} (eV)	-5.8880	-5.6995
E_{LUMO} (eV)	-2.1896	-2.0223
Energy gap ΔE (eV)	3.6984	3.6772
Dipole moment μ (D)	4.1222	3.1635
Ionization energy I (eV)	5.8880	5.6995
Electron affinity A (eV)	2.1896	2.0223
Electronegativity χ (eV)	4.0388	3.8609
Hardness η (eV)	1.8492	1.8386
Softness (σ) $(eV)^{-1}$	0.5408	0.5439
Fraction of electron transferred ΔN	0.0652	0.1140
Electrophylicity index ω	4.4105	4.0538
Total energy E_T (Ha)	-1168.6693	-963.9391

The optimized structures used to calculate global reactivity parameters and graphical representation of HOMO and LUMO orbitals were illustrated in **Figure 7**. This representation denotes that the electronic distribution extends over the entire surface of the molecule for HOMO orbitals of both compounds. For LUMO orbitals, this distribution occurs on the part where there are more heteroatoms (N, O) in each molecule. These observations relate that these heteroatoms share free electron pairs to form covalent bonds with aluminum.

It has been reported that an E_{HOMO} high value attests that the molecule can donate electrons to a suitable acceptor, while a low value of E_{LUMO} relates that the molecule is likely to accept electrons from the metal [43].

In this study, Table 3 examination exposes that BNIH has the highest E_{HOMO} value, indicating that during inhibition, BNIH can donate more electrons to aluminum than NBIH. This high electron donation capacity justifies its better inhibition performance than NBIH, as indicated by experimental results. Indeed, it has been proven that during

corrosion, the metal loses its electrons, so any compound capable of providing electrons in replacement can reduce its dissolution. In contrast, NBIH displays the lowest E_{LUMO} value, indicating that NBIH can readily accept electrons from metal compared to BNIH. This good electron acceptance suitability can be justified by the presence of two NO_2 substituents in its structure. These substituents would increase its inductive attractive effect.

Inhibitor	Optimized structures	HOMO Orbital	LUMO Orbital
NBIH		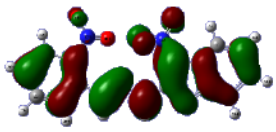	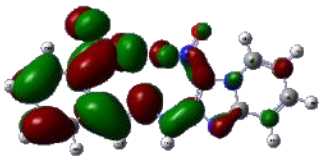
BNIH	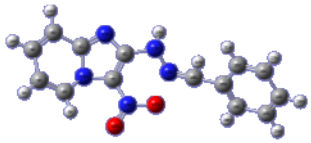	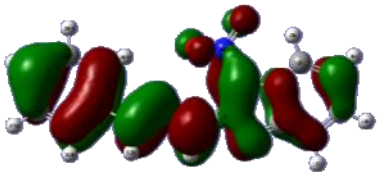	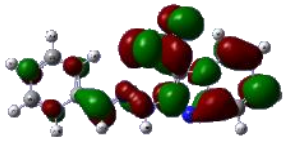

Figure 7 Optimized structures, HOMO, and LUMO Orbitals for tested molecules

The reactivity of a compound depends on its energy gap value (ΔE), a low ΔE value certifying that the molecule is highly reactive [44, 45]. Theoretical calculations indicate that BNIH has the lowest ΔE value, confirming its greater inhibition capacity obtained experimentally.

According to previous studies, several discrepancies have been reported in the correlation between dipole moment (μ) and inhibition efficiency (IE) [46, 47]. In this work, molecules tested inhibition efficiency of the molecules tested increases with decreasing dipole moment. Because of these numerous irregularities, no correlation can be established between dipole moment and the inhibition efficiency of the compounds studied.

The fraction of electrons transferred (ΔN) is a quantum chemical parameter that depends the electronegativities of an inhibitor and the metal. ΔN values of BNIH and NBIH are positive. These significant values state that aluminum electronegativity is greater than that of molecules. In this case, BNIH and NBIH can donate electrons to aluminum [48].This electron donation is confirmed by the low ionization energy (I) values obtained for both molecules. So BNIH and NBIH, which can to donate electrons to aluminum, can adsorb to its surface, creating a protective layer to amortize its dissolution in HCl.

In addition, the inhibition properties of a molecule depend on its hardness (η) and softness (σ) values [49]. The results indicate that BNIH has the lowest value of η and the highest value of σ. It emerges in this case that BNIH is more reactive than NBIH.

Accordingly, BNIH has the best inhibition efficiency, which corresponds well with the experimental data. NBIH electrophilicity index value (ω) is higher than that of BNIH, suggesting that NBIH is more electrophilic than BNIH [50], as indicated by the E_{LUMO} and E_{HOMO} values. These theoretical data confirm the good inhibition power of BNIH obtained experimentally. The DFT calculations listed in Table 3 highlight that BNIH has the highest total energy, which could explain its good inhibition performance.

Quantitative Structure-Property Relationship Simulation

QSPR approach was based on experimental inhibition efficiencies obtained at T=298K. The results obtained are listed in **Table 4**.

Table 4 IE values for inhibitors at 298K

Inhibitor	Concentration(mM)	IE(%)
NBIH	0.1	76.81
	0.3	82.03
	0.6	87.34
	0.8	91.56
BNIH	0.1	78.90
	0.3	83.12
	0.6	91.60

0.8	95.78

From equation 16 and based on the four concentrations (100μM, 300 μM, 600μM, 800μM), the sets of three quantum chemical parameters (x_1, x_2, x_3), and the corresponding inhibition efficiencies (I_1, I_2, I_3 et I_4) for each inhibitor obtained at 298K. A system of four equations with four unknowns (A, B, D, and E) has been obtained. Solving this system leads to A, B, D, and E values for each set of parameters used. These values are given in **Table 5**.

$$[100-I_1]C_1 * x_1 * A + [100-I_1]C_1 * x_2 * B + [100-I_1]C_1 * x_3 * D + [100-I_1]C_1 * E = I_1$$
$$[100-I_2]C_2 * x_1 * A + [100-I_2]C_2 * x_2 * B + [100-I_2]C_2 * x_3 * D + [100-I_2]C_2 * E = I_2$$
$$[100-I_3]C_3 * x_1 * A + [100-I_3]C_3 * x_2 * B + [100-I_3]C_3 * x_3 * D + [100-I_3]C_3 * E = I_3$$
$$[100-I_4]C_4 * x_1 * A + [100-I_4]C_4 * x_2 * B + [100-I_3]C_3 * x_3 * D + [100-I_4]C_4 * E = I_4$$

Table 5 Values of constants A, B, C, and E for each set of parameters

Inhibitor	Set of parameters	*A*	*B*	*D*	*E*
NBIH	$(E_{HOMO}, \Delta E, \chi)$	690.3479053	-1.40873X10^{13}	-4.22008X10^{11}	5.3805X10^{13}
	$(\Delta N, I, \eta)$	40394.8112	1.91376E+12	-9.73184X10^{12}	6.7279X10^{12}
	$(E_{HOMO}, E_{LUMO}, \omega)$	4.033X10^{13}	2.20584X10^{13}	4.79444X10^{13}	6.7279X10^{12}
	$(\sigma, \Delta E, A)$	1681.041815	-13159.46334	2359.31034	42593.92108
BNIH	$(E_{HOMO}, \Delta E, \chi)$	1213.879849	5.30261X10^{11}	-2.41269X10^{13}	9.12016X10^{13}
	$(\Delta N, I, \eta)$	-26386.98	-21.1	143667.3874	-261095.8239
	$(E_{HOMO}, E_{LUMO}, \omega)$	-6562.192802	-31.41304424	-1869.316442	-5871.763111
	$(\sigma, \Delta E, A)$	879.1666663	1589.725491	1211	-8772.88523

Table 6 R^2, SSE, and RMSE values

Inhibitor	Set of parameters	R^2	SSE	RMSE
NBIH	$(E_{HOMO}, \Delta E, \chi)$	0.9089	1281.95	17.90
	$(\Delta N, I, \eta)$	0.9251	2103.30	22.93
	$(E_{HOMO}, E_{LUMO}, \omega)$	0.9151	314.79	8.87
	$(\sigma, \Delta E, A)$	0.9052	287.05	8.47
BNIH	$(E_{HOMO}, \Delta E, \chi)$	0.9106	92.36	4.80
	$(\Delta N, I, \eta)$	0.9381	582.36	12.06
	$(E_{HOMO}, E_{LUMO}, \omega)$	0.9404	593.37	12.17
	$(\sigma, \Delta E, A)$	0.9209	31.01	2.78

Table 6 lists the values of correlation coefficients and statistical parameters. Analysis of the values recorded in Table 6 reveals that all sets of parameters selected lead to a satisfactory correlation between theoretical and experimental efficiency values (R^2>0.9).Furthermore, a set of parameters $(\sigma, \Delta E, A)$, which presents low SSE and RMSE values for NBIH and BNIH, would be the most appropriate for describing the behavior of the inhibitors studied. BNIH has the lowest statistical parameter values, confirming the high IE values obtained experimentally. In addition, this model will enable to predict the inhibition efficiency for each compound studied, based on concentrations and a set of parameters $(\sigma, \Delta E, A)$. This prediction will facilitate other organic inhibitor's design [51-53]. Theoretical data (DFT and QSPR) are consistent with experimental results. Some previous works have found a similar convergence [48, 54]. **Figure 8** illustrates the correlation between experimental and theoretical data.

Mechanism of inhibition of inhibitors tested

Quantum chemical descriptors mention that molecules can donate and accept electrons from metal. Each inhibitor is protonated in the hydrochloric acid solution. The equation for this reaction is as follows:

$$Ni + HCl \rightleftarrows [NiH]^+ + Cl^- \qquad \{1\}$$

Aluminum also loses electrons in hydrochloric acid solution:

$$Al + 6H^+ \rightarrow 2Al^{3+} + 3H_2 \qquad \{2\}$$

Electrostatic interactions (physisorption) are created between Cl^- ions located on the metal surface and the protonated form of each inhibitor. As a result, a protective layer resulting from these interactions attaches to aluminum surface, isolating it from the aggressive medium. These interactions are strong at low temperatures, which justifies the high inhibition efficiencies at these temperatures.

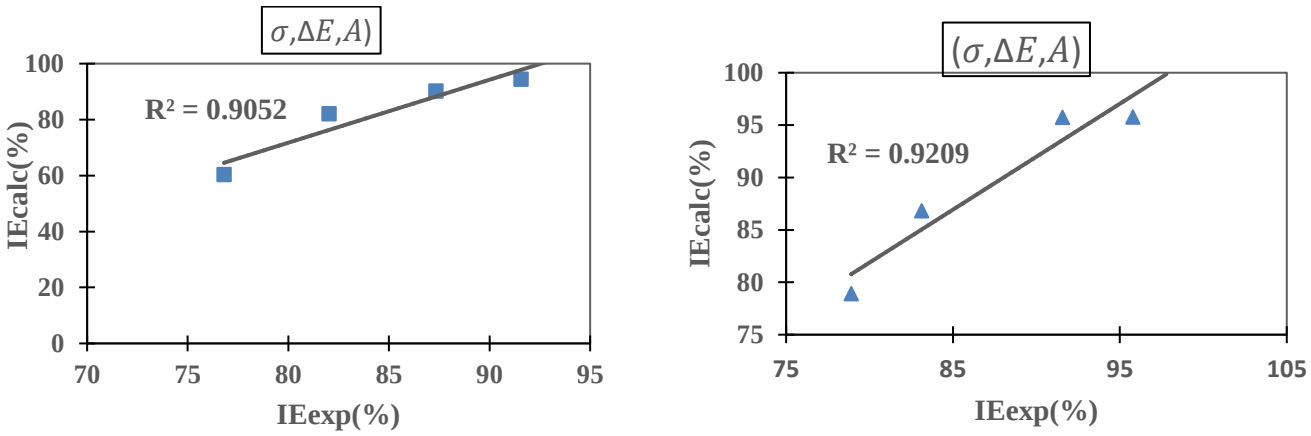

(a) (b)

Figure 8 Calculated versus experimental inhibition efficiency of NBIH (a) and BNIH (b)

At higher temperatures, aluminum loses more electrons. The values of quantum chemical descriptors such as (ΔN), E_{HOMO}, E_{LUMO}, and energy (ΔE) displayed by each inhibitor indicate that electrons are exchanged between inhibitor and metal. These electron exchanges are favored by the presence of free electron pairs of heteroatoms (N, O) as well as the π electron system of aromatic rings. These exchanges lead to covalent bonds (chemisorption) formation, which are unable to compensate for the electron deficit that occurs at higher temperatures. These data confirm the low inhibition efficiencies obtained at these temperatures.

Conclusion

Gravimetric and theoretical data obtained from this study lead to the following conclusions:

- BNIH and NBIH have good inhibition properties against aluminum corrosion in 2M hydrochloric acid.
- BNIH and NBIH inhibition efficiency increases with concentration and decreases with increasing temperature.
- BNIH inhibition efficiency is higher than that of NBIH, which is justified by the presence of two NO_2 substituents in NBIH.
- Both compounds adsorb to the aluminum surface according to Villamil's model.
- Thermodynamic quantities for adsorption and activation show that the adsorption of molecules is spontaneous and occurs both chemically and physically, but the process is dominated by physical adsorption and is accompanied by an increase in disorder as the reactants transform into the activated complex.
- Quantum chemical parameters calculated using DFT show that BNIH and NBIH have good electron acceptor and donor properties.
- DFT calculations confirm that BNIH has the best inhibition performance.
- QSPR simulation relates that the set of quantum chemical parameters ($\sigma, \Delta E, A$) is likely to correlate experimental and theoretical data.
- Finally, the experimental and theoretical results obtained are consistent and convergent.

References

[1] Y. Boughoues, M. Benamira, L. Messaadia, N. Ribouh. Adsorption and corrosion inhibition performance of some environmental friendly organic inhibitors for mild steel in HCl solution via experimental and theoretical study. Colloids and Surfaces A: Physicochemical and Engineering Aspects, 2020, 593: 124610

[2] C. Verma, E.E. Ebenso, M. Quraishi. Ionic liquids as green and sustainable corrosion inhibitors for metals and alloys: An overview. Journal of Molecular Liquids, 2017, 233: 403-414.

[3] S.H. Zaferani, M. Sharifi, D. Zaarei, M.R. Shishesaz. Application of eco-friendly products as corrosion inhibitors for metals in acid pickling processes–A review. Journal of Environmental Chemical Engineering, 2013, 1: 652-657.
[4] A. Kumari, M.K. Jha, J.-c. Lee, R.P. Singh. Clean process for recovery of metals and recycling of acid from the leach liquor of PCBs. Journal of Cleaner Production, 2016, 112: 4826-4834.
[5] S. Satpati, S. Kr, A. Saha, P. Suhasaria, D. Sukul Banerjee. Adsorption and anticorrosion characteristics of vanillin Schiff bases on mild steel in 1 M HCl: experimental and theoretical study. RSC Advances, 2010, 10: 9258–9273.
[6] R. Padash, G. S. Sajadi, A. H. Jafari, E. Jamalizadeh, A. Shokuhi Rad. Corrosion control of aluminum in the solutions of NaCl, HCl and NaOH using 2,6-dimethylpyridine inhibitor: Experimental and DFT insights. Materials Chemistry and Physics,2020, 244: 122681.
[7] S. Bashir, V. Sharma, G.Singh et al. Electrochemical Behavior and Computational Analysis of Phenylephrine for Corrosion Inhibition of Aluminum in Acidic Medium. Metallurgical and Materials Transactions A, 2019, 50: 468–479.
[8] R. Padash, G. S. Sajadi, A. H. Jafari, E. Jamalizadeh,A. S. Rad. Corrosion control of aluminum in the solutions of NaCl, HCl and NaOH using 2,6-dimethylpyridine inhibitor: Experimental and DFT insights. Materials Chemistry and Physics, 2020, 244: 122681.
[9] J. Wang, J. Liu, X. Wang. The anticorrosive applications of anionic surfactant on AA2024-T3 aluminum alloy in alkaline medium: Experimental and theory. Journal of Molecular Structure, 2023, 1275: 134612.
[10] Q. Wang, H. Li. Study on anodic oxidation of 2099 aluminum lithium alloy and sealing treatment in environmental friendly solutions. International Journal of Electrochemical Science, 2023, 18(7): 100186.
[11] B.J. Usman, F. Scenini, M. Curioni. The effect of exposure conditions on performance evaluation of post-treated anodic oxides on an aerospace aluminium alloy: comparison between salt spray and immersion testing. Surface and Coatings Technology.2020, 399: 126157
[12] R. Wang, L. Wang, H.Chunying, L.Min Lu. Studies on the sealing processes of corrosion resistant coatings formed on 2024 aluminum alloy with tartaric-sulfuric anodizing. Surface and Coatings Technology, 2019, 36025: 369-375.
[13] M. Chafiq, A. Chaouiki,H. Lgaz et al. New spirocyclopropane derivatives: synthesis and evaluation of their performances toward corrosion inhibition of mild steel in acidic media. Research on Chemical Intermediates,2020, 46: 2881–2918.
[14] A. Fouda, S. Al-Sarawy, A. Sh, F. Ahmed, H.M. El-Abbasy.Corrosion inhibition of aluminum 6063 using some pharmaceutical compounds. Corrosion science, 2009, 51: 485-492
[15] B. Benzidia, M. Barbouchi, M. Rehioui, H. Hammouch, H. Erramli, N. Hajjaji. Aloe vera mucilage as an eco-friendly corrosion inhibitor for bronze in chloride media: Combining experimental and theoretical researches, Journal of King Saud University – Science, 2023, 35(11): 102986.
[16] B. U.Ugi, I. E.Uwah, N. U. Ukpe. (2014). Inhibition and Adsorption impact of Leave Extracts of Cnidoscolus Aconitifolius on Corrosion of Aluminium Sheet in 1 M HCl Medium. Journal of Applied Sciences and Environmental Management, 2014, 18: 319-325
[17] H.R. Khalid, A. A. Khadom, S. H. Abbas, F. Al-azawi Khalida, H. B. Mahood. Optimization studies of expired mouthwash drugs on the corrosion of aluminum 7475 in 1 M hydrochloric acid: Gravimetrical, electrochemical, morphological and theoretical investigations. Results in Surfaces and Interfaces,2023, 13: 100165,
[18] H. Lgaz, R. Salghi, S. Jodeh, B. Hammouti. Effect of clozapine on inhibition of mild steel corrosion in 1.0 M HCl medium. Journal of Molecular Liquids, 2017, 225: 271-280.
[19] Z. A. Kaplancikli, G. Turan-Zitouni, A. Özdemr, G. Revial. Synthesis and anticandidal activity of some imidazopyridine derivatives. Journal of Enzyme Inhibition and Medicinal Chemistry, 2008, 23(6): 866–870
[20] Damghani, T., Moosavi, F., Khoshneviszadeh, M. et al. Imidazopyridine hydrazone derivatives exert antiproliferative effect on lung and pancreatic cancer cells and potentially inhibit receptor tyrosine kinases including c-Met. Science Report, 2021, 11: 3644.
[21] M.J. Frisch, G.W. Trucks, H.B. Schlegel, G.E. Scuseria, M.A. Robb, J.R. Cheeseman, G. Scalmani, V. Barone, B. Mennucci, G.A. Petersson, H. Nakatsuji, M. Caricato, X. Li, H.P. Hratchian, A.F. Izmaylov, J. Bloino, G. Zheng, J.L. Sonnenberg, M. Hada, M. Ehara, K. Toyota, R. Fukuda, J. Hasegawa, M. Ishida, T. Nakajima, Y. Honda, O. Kitao, H. Nakai, T. Vreven, J.A. Montgomery Jr., J.E. Peralta, F. Ogliaro, M. Bearpark, J.J. Heyd, E. Brothers, K.N. Kudin, V.N. Staroverov, R. Kobayashi, J. Normand, K. Raghavachari, A. Rendell, J.C. Burant, S.S. Iyengar, J. Tomasi, M. Cossi, N. Rega, J.M. Millam, M. Klene, J.E. Knox, J.B. Cross, V. Bakken, C. Adamo, J. Jaramillo, R. Gomperts, R.E. Stratmann, O. Yazyev, A.J. Austin, R. Cammi, C. Pomelli, J.W.

Ochterski, R.L. Martin, K. Morokuma, V.G. Zakrzewski, G.A. Voth, P. Salvador, J.J. Dannenberg, S. Dapprich, A.D. Daniels, Ö. Farkas, J.B. Foresman, J.V. Ortiz, J. Cioslowski, D.J. Fox, Gaussian 09, Revision D.01, Gaussian, Inc., Wallingford CT, 2009

[22] A. D. Becke, Density-functional thermochemistry. The effect of the exchange-only gradient correction.The journal of chemical physics, 1992, 96: 2155–2160

[23] R. G. Parr, W. Yang. Density functional approach to the frontier-electron theory of chemical reactivity. Journal of the American Chemical Society, 1984,106: 4049-4050,

[24] D. Kumara, N. Jain, B. Rai. Amino acids as copper corrosion inhibitors: A density functional theory approach. Applied Surface Science, 2020, 514: 145905

[25] B. Yang, L. Yizhen, Z. Zhang, H. Xinying, Y. Zhu. Anticorrosion mechanism of natural acidic amino acids on steel in chloride solution: Experimental, theoretical and machine learning approaches. Journal of Building Engineering, 2023, 79: 107801

[26] M.J.S. Dewar, E.G Zoebisch, E.F. Healy, J.P. Stewart. Development and Use of Quantum Mechanical Molecular Models, 76, AM1: A New General Purpose Quantum Mechanical Molecular Model. Journal of the American Chemical Society, 1985, 107: 3902-3909.

[27] M.R. Albayati, S. Kansız, N. Dege, Savaş. Kaya, R. Marzouki, H. Lgaz, R. Salghi, I.H. Ali, M.M. Alghamdi, M. Chung Ill. Synthesis, crystal structure, Hirshfeld surface analysis and DFT calculations of 2-[(2,3-dimethylphenyl)amino]-N'-[(E)-thiophen-2-ylmethylidene]benzohydrazide. Journal of Molecular Structure,2020,1205: 127654.

[28] C. Morell, A. Grand, A. Toro-Labbé. New Dual Descriptor for Chemical Reactivity. Journal of Physical Chemistry A, 2005,109: 205-212.

[29] J.I. Martínez-Araya. Why Is the Dual Descriptor a More Accurate Local Reactivity Descriptor than Fukui Functions? Journal of Mathematical Chemistry, 2015, 5: 451-465.

[30] T.W. Quadri, L. O. Olasunkanmi, O. E. Fayemi, H. Lgaz, O. Dagdag, E. M. Sherif, A. A. Alrashdi, E. D. Akpan, H. Lee, E. E. Ebenso. Computational insights into quinoxaline-based corrosion inhibitors of steel in HCl: Quantum chemical analysis and QSPR-ANN studies. Arabian Journal of Chemistry, 2022,15(7): 103870.

[31] I. Lukovits, E.F. Kalman. Corrosion Inhibitors—Correlation between Electronic Structure and Efficiency, Corrosion (NACE), 2001, 57(1): 3-8.

[32] H.R.B. Beda, M.A. Tigori, D. Donourou P.M. Niamien. Anticorrosive Properties of Theophylline on Aluminum Corrosion in 1 M HCl: Experimental, and Computational Assessment of Iodide Ions Synergistic Effect. Current Physical Chemistry 2021,11(3):227-242.

[33] M.M. Motawea, S. Melhi. Electrochemical and computational studies of an expired vilazodone Drug as environmentally safe corrosion inhibitor for aluminum in chloride medium, Journal of the Indian Chemical Society, 2023,100(6): 101013,

[34] R. F. V. Villamil, P. Corio, J.C. Rubin, S. M. L. Agostinho. Effect of sodium dodecylsulfate on copper corrosion in sulfuric acid media in the absence and presence of benzotriazole. Journal of Electroanalytical Chemistry, 1999,472(2): 112-116.

[35] K. H. Rashid, A. A. Khadom, S. H. Abbas, K. F. Al-azawi, H. B. Mahood. Optimization studies of expired mouthwash drugs on the corrosion of aluminum 7475 in 1 M hydrochloric acid: Gravimetrical, electrochemical, morphological and theoretical investigations. Results in Surfaces and Interfaces,2023,13: 100165.

[36] M. D. Allah, M. El Hefnawy, S. A. Elhamed. Experimental investigation of the corrosion inhibition of Aluminum by three novel anionic surfactants as green inhibitors in HCl solution. Chemical Data Collections, 2023, 45: 101033.

[37] A. Benallal, M. Rbaa, Z. Rouifi et al. Quinoxaline Derivatives as Newly Acid Corrosion Inhibitors for Mild Steel: Synthesis, Electrochemical, and Theoretical Investigations. Journal of Bio-and Tribo-Corrosion, 2023, 9, 30.

[38] M. Abdallah, A. Al Bahira, H.M Altass, A. Fawz, N. El Guesmi, A.S. Al-Gorair, F.B. Warad, A. Zarrouk. Anticorrosion and Adsorption Performance of Expired Antibacterial Drugs on Sabic Iron Corrosion in HCl Solution: Chemical, Electrochemical and Theoretical Approach. Journal of Molecular Liquids, 2021, 330: 115702.

[39] M. Dibetsoe, L. O. Olasunkanmi, O. E. Fayemi, S. Yesudass, B. Ramaganthan, I. Bahadur, A. S. Adekunle, M. M. Kabanda, E. E. Ebenso. Some Phthalocyanine and Naphthalocyanine Derivatives as Corrosion Inhibitors for Aluminium in Acidic Medium: Experimental, Quantum Chemical Calculations, QSAR Studies and Synergistic Effect of Iodide Ions. Molecules, 2015, 20: 15701-15734.

[40] S. Monikandon, D. Kesavan, R. Marimuthu. Eco-friendly inhibitor for corrosion of TMT rod in marine

environment. Materials Today: Proceedings,2022,58(3): 898-901
[41] O.Id El Mouden, M.E.Belghiti et al Anti-corrosive properties of two new green heterocyclic azole derivatives on C38 steel in 1 M (HCl) medium, experimental and theoretical study. Results in Chemistry, 2023, 5: 100641.
[42] A.K. Singh, S. Mohapatra, B. Pani. Corrosion inhibition effect of Aloe Vera gel: Gravimetric and electrochemical study. Journal of Industrial and Engineering Chemistry, 2016, 33: 288-297.
[43] J. Zeng, Y. Gan, Z. Xu, H. Zhu, B. Tan, W. Li. Adsorption films based on indazole derivatives for application to protect Cu in sulfuric acid: Experimental and theoretical approaches. Journal of the Taiwan Institute of Chemical Engineers, 2023, 151: 105134,
[44] Y. Ting, S. Zhang, F. Li, Q. Yujie, L. Lansi, F. Denglin, W. Yanan,C. Jida, L. Wenpo, T. Bochuan. Investigation of imidazole derivatives as corrosion inhibitors of copper in sulfuric acid: Combination of experimental and theoretical researches. Journal of the Taiwan Institute of Chemical Engineers, 2020, 106: 118-129
[45] M. Mobin, I. Ahmad, M. Murmu, P. Banerjee, R. Aslam. Corrosion inhibiting properties of polysaccharide extracted from Lepidium meyenii root for mild steel in acidic medium: Experimental, density functional theory, and Monte Carlo simulation studies. Journal of Physics and Chemistry of Solids, 2023: 111411.
[46] A. Zarrouk, B. Hammouti, D. Ali,B. Mohammed, Z. Hassan, S. Boukhris, S.A. Salem. A theoretical study on the inhibition efficiencies of some quinoxalines as corrosion inhibitors of copper in nitric acid. Journal of Saudi Chemical Society, 2014, 18, 450-55.
[47] H. Rajesh, P. Dwarika, S. Akhil, K. Raman. Experimental and theoretical studies of Ficus religiosa as green corrosion inhibitor for mild steel in 0.5 M H2SO4 solution. Sustainable Chemistry and Pharmacy, 2018, 9: 95-105.
[48] S. Bashir,V. Sharma, G. Singh et al. Electrochemical Behavior and Computational Analysis of Phenylephrine for Corrosion Inhibition of Aluminum in Acidic Medium. Metallurgical and Materials Transactions A, 2019,50: 468–479.
[49] C. Verma, V.S. Saji, M.A. Quraishi, E.E. Ebenso. Pyrazole derivatives as environmental benign acid corrosion inhibitors for mild steel: Experimental and computational studies. Journal of Molecular Liquids Volume, 2020, 298: 111943,
[50] R.G. Parr, L.Sventpaly, Liu, S. Electrophilicity index. Journal of the American Chemical Society, 1999, 121(9): 1922-1924.
[51] M. Ghamali, S. Chtita, R. Hmamouchi, A. Adad, M. Bouachrine, T. Lakhlifi, The inhibitory activity of aldose reductase of flavonoids compounds. Combining DFT and QSAR calculations. Journal of Taibah University for Science, 2016, 10(4): 534-542.
[52] E. E. Ebenso, D. A. Isabirye, N. O. Eddy. Adsorption and Quantum Chemical Studies on the Inhibition Potentials of Some Thiosemicarbazides for the Corrosion of Mild Steel in Acidic Medium. International Journal of Molecular Sciences, 2010, 11: 2473-2498
[53] M. Akrom, S. Rustad, A. G. Saputro, H. K. Dipojono. Data-driven investigation to model the corrosion inhibition efficiency of Pyrimidine-Pyrazole hybrid corrosion inhibitors. Computational and Theoretical Chemistry, 2023, 1229: 114307.
[54] A. Anees Khadom, M. M. Kadhim, R. A. Anaee, H. B. Mahood, M. S. Mahdi, A. W. Salman.Theoritical evaluation of Citrus Aurantium leaf extract as green inhibitor for chemical and biological corrosion of mild steel in acidic solution: Statistical, molecular dynamics, docking, and quantum mechanics study.Journal of Molecular Liquids,2021,343 : 116978.

Publication History
Received 20.02.2024
Revised 28.03.2024
Accepted 28.03.2024
Online 31.03.2024